MALAYSIAN JOURNAL OF ANALYTICAL SCIENCES
Published by The Malaysian Analytical Sciences Society
ISSN 1394 - 2506

INVESTIGATION ON OPTICAL AND PHOTOELECTROCHEMICAL PROPERTIES OF SELF-ASSEMBLED TITANIA NANOTUBE ARRAYS PREPARED BY ANODIZATION

(Penyiasatan Sifat Optik dan Fotoelektrokimia Swahimpunan Nanotiub Titania Bertatasusunan yang Disediakan Melalui Penganodan)

Lim Ying Chin[1]*, Zulkarnain Zainal[2], Mohd Zobir Hussein[3], Tan Wee Tee[2]

[1]School of Chemistry and Environment, Faculty of Applied Sciences,
Universiti Teknologi MARA (UiTM), 40450 Shah Alam, Selangor, Malaysia
[2]Department of Chemistry, Faculty of Science
[3]Advanced Materials and Nanotechnology Laboratory, Institute of Advanced Technology (ITMA)
Universiti Putra Malaysia, 43400 UPM Serdang, Selangor, Malaysia

**Corresponding author: limyi613@salam.uitm.edu.my*

Received: 9 December 2014; Accepted: 16 November 2015

Abstract

Well ordered and vertically oriented titania nanotubes (TNT) are of great scientific interest due to their high surface area, fewer interfacial grain boundaries and excellent charge transfer between interfaces; all are critical properties in photoelectrochemical and photocatalysis application. In this study, self-assembled TNT electrodes were synthesized by anodization of pure Ti in 0.5 wt.% NH_4F solution (NH_4F/H_2O), in mixture of aqueous-organic solution (NH_4F/H_2O/EG) and in an organic solution (NH_4F/EG). Choice of electrolytic medium has an influence on the crystalline structure, regularity, elemental composition and band gap of TNT. All the samples showed a red shift and stronger absorption in the wavelength between 500-700 nm ascribed to the surface colour and increase crystallinity upon calcination. TNT formed in NH_4F/H_2O solution has the highest direct band gap of 3.34 eV due to quantization effect. From Liner Sweep Photovoltammetry analysis, the lowest photocurrent was recorded for TNT anodized in NH_4F/H_2O and a twofold and fivefold increase on the magnitude of photocurrent was obtained for those formed in NH_4F/H_2O/EG and NH_4F/EG solution, respectively. Hence, highest photoefficiency of 2.79 % was recorded for TNT formed in NH_4F/EG probably due to the formation of longer length tube.

Keywords: titania, nanotube, anodization, photoefficiency, band gap energy

Abstrak

Nanotiub titanium dioksida yang bertertib rapi dan berorientasi mencancang (TNT) telah menarik perhatian disebabkan luas permukaan yang tinggi, sempadan butiran antara muka yang rendah dan pemindahan cas yang cemerlang di antara muka, yang mana semua ini merupakan ciri – ciri kritikal dalam aplikasi fotoelektrokimia and fotopemangkinan. Dalam kajian ini, swahimpunan TNT telah disintesis melalui penganodan plat titanium tulen dalam larutan 0.5 wt.% NH_4F (NH_4F/H_2O), campuran larutan akua-organik (NH_4F/EG/H_2O) dan larutan organik (NH_4F/EG). Pilihan media elektrolisis memberi kesan ke atas struktur hablur, keteraturan, komposisi unsur dan julang jalur TNT. Semua sampel mempamerkan anjakan merah dan penyerapan yang lebih kuat dalam julat gelombang 500 – 700 nm disebabkan warna permukaan sampel dan peningkatan kehabluran selepas pemanasan. Dari analisis fotovoltammetri pengimbasan linear, TNT yang teranod dalam larutan NH_4F/H_2O mencatatkan fotoarus yang terendah manakala peningkatan lipat ganda dua dan ganda lima dalam magnitud fotoarus boleh didapati untuk TNT yang teranod dalam larutan NH_4F/H_2O/EG dan NH_4F/EG. Oleh yang demikian, TNT yang dibentuk dalam latutan NH_4F/EG mencatatkan kecekapan foto yang tertinggi sebanyak 2.79 % mungkin disebabkan oleh pembentukan tiub yang lebih panjang.

Kata kunci: titania, nanotiub, penganodan, kecekapan foto, jalur jurang tenaga

Introduction

Titania (TiO_2) appears to be the most promising material to be used in photoelectrochemical applications due to its high efficiency, low cost, chemical inertness and photostability [1 – 4]. However, bulk TiO_2 materials have low surface area and therefore exhibit low adsorption property. Moreover, fast recombination rate of the photogenerated charge carriers deteriorate the performance of such materials especially in photoelectrochemical applications. In order to overcome such problems, much effort has been focused on fabrication of highly efficient materials with suitable architecture to minimize the recombination of electron-hole pairs. In this context, formation of highly ordered and oriented nanotubular or porous geometry is advantageous due to high surface-to-volume ratio and short diffusion path within enclosed nanoscale compartment [5]. Self-organized growth of TiO_2 nanotube arrays are of great interest due to its unique physical properties including larger surface area in a small geometrical area, fewer interfacial grain boundaries and superior charge transport, of which all are important properties governing its performance as photoanode in a photoelectrochemical cell. Therefore, the study aimed at synthesizing titania nanotubes in various electrolytic compositions in order to investigating the effects of electrolyte nature on the microstructure, optical and photoelectrochemical performance of the synthesized TNT.

Materials and Methods

Fabrication of titania nanotube arrays

A Ti foil (99.7%, Sigma Aldrich) was used for producing vertically oriented nanotubes. Prior to anodization, the Ti foils were cleaned by sonication in acetone, isopropanol, and deionized (DI) water respectively, followed by subsequent etching in 6 M HNO_3. They were then rinsed with DI water and dried in air. An electrochemical cell with a two-electrode configuration was used. The Ti foil served as the working electrode and high density graphite was used as the counter electrode and they were separated by approximately 2 cm. All the experiments were driven by a DC power source (Consort Mini, Cleaver Scientific Ltd) and were carried out at room temperature in three different types of electrolytes for 2 hours to form TNT. The composition of the three electrolyte solutions and voltage used for anodization were summarized in Table 1. After the anodization process, the samples were rinsed with DI water and dried in air. Subsequently, they were calcined at 500 ^oC in air for 2 hours with a heating rate of 2 ^oC/minutes. The resultant calcined TNT are hereinafter designated as C5TNT/H_2O, for the 0.5 wt% NH_4F solution adjusted to pH 4, C5TNT/EGH_2O, for the mixture of ethylene glycol containing 50 vol.% H_2O and 0.5 wt.% NH_4F and C5TNT/EG, for ethylene glycol containing 0.5 wt.% NH_4F. For comparison, the as-anodized samples without heat treatment were produced and were designated as AOTNT/H_2O, AOTNT/EGH_2O and AOTNT/EG, respectively.

Table 1. Summary of electrolyte compositions and voltage used producing TNT during anodization

Samples	Electrolyte composition	Voltage / V
TNT/H_2O	0.5 wt.% NH_4F adjusted to pH 4	20
TNT/EGH_2O	0.5 wt.% NH_4F + ethylene glycol + 50 vol.% H_2O	20
TNT/EG	0.5 wt.% NH_4F + ethylene glycol	65

Characterization of titania nanotube arrays

Phase identification was carried out using an X-ray diffractometer (XRD, Shimadzu D6000) with Cu K_α radiation (λ= 1.5406 Å). The morphology of the samples was characterized on TEM Hitachi H-1700 operating at an accelerating voltage of 200 kV. Quantitative measurements were done using image analysis software (Image J). Energy dispersive analysis of x-rays (EDX) was performed on JOEL FESEM JSM-7600F JOEL, Japan attached with Oxford INCA Energy 200 EDX to determine the purity and elemental composition in the as-anodized and

calcined samples. The optical absorbance behavior of TNT was characterized using a diffuse reflectance UV-VIS-NIR spectrophotometer (Model: UV-3600, Shimadzu Corporation, Kyoto, Japan) equipped with an integration sphere. $BaSO_4$ was used as a reflectance standard. The band gap energy (E_g) can be calculated using the absorbance data obtained following the Tauc Plot relation (Equation 1):

$$\alpha h\nu = A(h\nu - E_g)^n \quad (1)$$

where α is the absorption coefficient, h is the Planck's constant, ν is the wavenumber and A is a constant. The "n" depends on the types of band-to-band transition (for titania, n=2 for a direct band gap and n= ½ for a indirect transition between bands). The band gap energy could be obtained by extrapolating the straight line in the plot of $\alpha^{1/2}$ or $\alpha h\nu^2$ against $h\nu$ to the base line where $\alpha^{1/2}$ or $\alpha h\nu^2 = 0$. Thus, the E_g is equivalent to $h\nu$.

Photoelectrochemical test

Photoelectrochemical response of TNT was demonstrated using a three-electrode system with the synthesized TNT as the working electrode, a platinum wire as the counter electrode, and Ag/AgCl as the reference electrode. The photocurrent was measured with a scanning potentiostat (μAutolab type III) during a voltage sweep from +2.0 to –0.2 V with the sweep rate of 20 mV/s in 10 ppm methyl orange with 0.1 M KCl as the supporting electrolyte. All the potentials were quoted against Ag/AgCl reference electrode. A tungsten halogen lamp (300 W, 120 V) was used for illuminating the TNT samples and the light was intermittently chopped at a constant frequency to evaluate both the photocurrent and dark current. A UV lamp (B-100AP) with the incident power of 11 mW/cm^2 was used to evaluate the efficiency of photocurrent generated by TNT prepared in different electrolytic medium and the radiation source was placed 15 cm away from the cell. The solution used was 0.1 M KOH

Results and Discussion

Electrolyte composition is an important parameter influencing the structure, morphology and geometry (and thus the specific surface area) of the resulted nanotubes. The crystallinity and the isomorphs of TNT are critical in influencing their properties and potential applications. Figure 1 illustrates the XRD patterns of TNT as a function of electrolytic medium. No peak shift was observed as a function of electrolytic medium. For TNT/H_2O, a mixture of anatase at $2\theta = 25.4^o$ (JCPDS No. 21-1272) and rutile at $2\theta = 27.6^o$ (JCPDS No. 21-1276) was observed after calcination at 500 ^oC. As opposed to TNT/H_2O, only pure anatase phase at $2\theta = 25.4^o$, 38.0^o, 48.2^o, 54.0^o and 55.2^o corresponding to (101), (004), (200), (105) and (211) plane, respectively was obtained for TNT/EG and TNT/EGH_2O upon calcination at 500 ^oC as shown in Figure 1 (b-c). Our finding is in contradiction with the work reported by other researchers that the crystalline structures remained unaffected with different electrolytic media [6, 7]. It is also discernible that the (101) reflection exhibited greatest intensity as compared to the other anatase peaks for all samples, demonstrating the preferred growth orientation for nanotubes at this plane. For TNT/EG sample, almost tenfold increase on the intensity magnitude of (101) reflection compared to TNT/H_2O and a threefold increase for TNT/EGH_2O sample, probably ascribed to increase in length for samples prepared in different electrolytic medium.

TEM analysis was performed to gain information on the microstructure of the sample. Figure 2 shows the TEM image of all samples. Apparently, a single nanotube consisted of a closed bottom with a barrier layer thickness of 37 nm and ripples on sidewall were obtained in NH_4F/H_2O solution. Same observation on the formation of ripples was obtained for TNT/EGH_2O. These ripples could be formed due to current fluctuations occurred during anodization process. In contrast, well-dispersed and straight nanotubes with uniform wall thickness and smooth tube wall throughout the length of the nanotubes can be observed for TNT formed in NH_4F/EG. Therefore, the electrolyte composition is a crucial factor determining the morphology of the outer wall where ripples are observed in nanotubes grown in aqueous electrolytes, whereas nanotubes prepared in ethylene glycol can be either smooth or are having ripples depending on the water content (50 vol. % in this study).

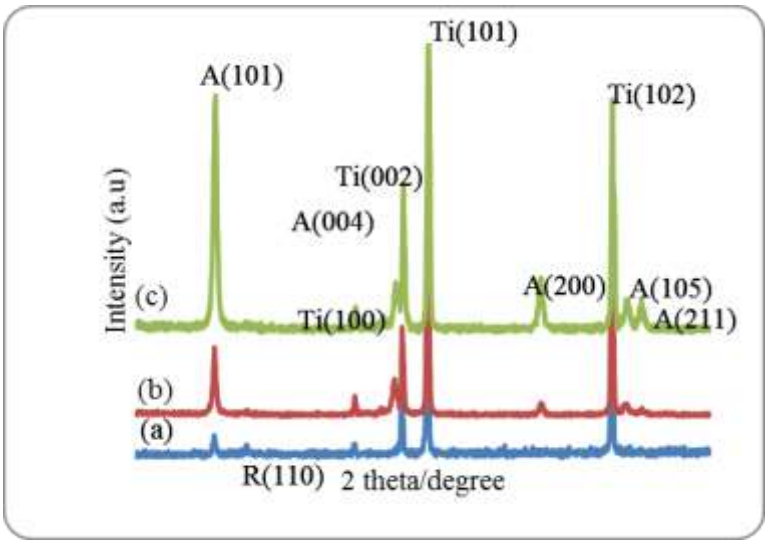

Figure 1. XRD patterns of calcined TNT synthesized at 20 V in different electrolytic medium with (a) NH_4F/H_2O (b) NH_4F/EG and (c) $NH_4F/EG/H_2O$ solution. A, R and Ti represent anatase, rutile and titanium, respectively

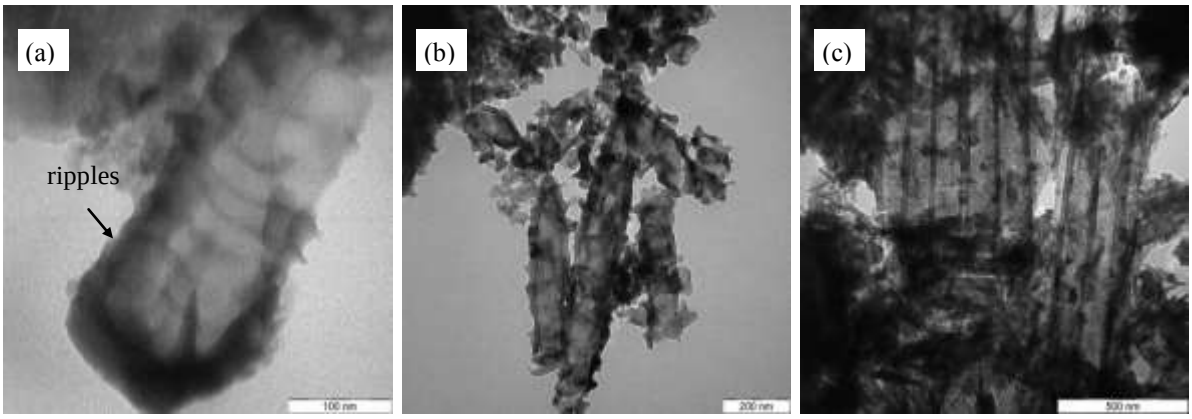

Figure 2. TEM images for (a) TNT/H_2O (b) TNT/EGH_2O and (c) TNT/EG

EDX analysis was done on blank Ti plate, as-anodized TNT and their calcined counterparts. The detailed compositions of the samples before and after calcination are shown in Table 2. For blank Ti, only Ti element was detected and C peak observed is due to carbon tape holding the sample. Evidently, Ti, O and F are found in the spectrum for $AOTNT/H_2O$, $AOTNT/EGH_2O$ and AOTNT/EG, with trace of carbon from the ethylene glycol observed for AOTNT/EG sample. The fluorine observed is due to the NH_4F added in the solution, which acts as a pore initiating agent. Calcination at 500 ^oC leads to a complete loss of the fluorine for C5TNT/EG and thus it is free from fluoride content and this result is similar with the work reported by Sreekantan et al. [8]. However, traces of F still can be detected for $C5TNT/H_2O$ and $C5TNT/EGH_2O$ but with almost negligible amount, indicating that the F is precipitated on the surface of sample during anodization and not incorporated into the TiO_2 lattice. In addition, all samples showed an increase in Ti and O content upon calcination. The molar ratio of Ti to O for calcined samples was close to the stoichiometric proportion, suggesting the samples were TiO_2.

For TNT/EG sample, a carbon rich layer could be probably obtained due to the voltage induced decomposition of the ethylene glycol as high voltage (65 V) is used during anodization of Ti. Therefore, higher C content (2.33 wt.%) was observed for AOTNT/EG sample. However, no C uptake from the solution occurs for C5TNT/EG given the C weight percent present is comparable to the blank Ti plate upon calcination at 500 ^{o}C. This result indicates that C from the ethylene glycol in AOTNT/EG could be easily removed via thermal treatment.

Table 2. Elemental analysis for Ti, as-anodised TNT and calcined TNT/H_2O, TNT/EGH_2O and TNT/EG

Sample	Weight percent (%)			
	Ti	O	C	F
Ti	99.44	-	0.45	-
AOTNT/H_2O	58.22	31.27	-	10.51
AOTNT/EGH_2O	51.20	38.53	-	10.27
AOTNT/EG	46.71	35.90	2.33	15.06
C5TNT/H_2O	61.83	36.11	-	2.06
C5TNT/EGH_2O	53.30	44.22	-	2.48
C5TNT/EG	63.11	36.60	0.29	-

Figure 3 shows the diffuse reflectance UV-Vis absorbance of both the as-anodized and calcined TNT prepared in different electrolytic medium. The absorbance response for AOTNT/H_2O, AOTNT/EGH_2O and AOTNT/EG exhibited lower absorption in the visible region, whereas the calcined counterparts showed a red shift and stronger absorption in the wavelength between 500−750 nm, with exception for C5TNT/EGH_2O. This can be attributed to the surface color and changes in crystalline structure of TNT. Generally, the color of C5TNT/H_2O was yellowish, dark green for C5TNT/EGH_2O and dark grey green for C5TNT/EG, respectively. In contrast, the as-anodized films were bright green, bright purple and bright grey for AOTNT/H_2O, AOTNT/EGH_2O and AOTNT/EG, respectively and this causes more adsorption in ultraviolet region and more reflection in the visible region. As shown in Figure 2, the absorption onset for C5TNT/H_2O, C5TNT/EGH_2O and C5TNT/EG was around 370, 380 and 390, respectively which was probably caused by increasing anatase content after thermal treatment. This is consistent with the changes in crystalline structure observed in XRD scan (Figure 1).

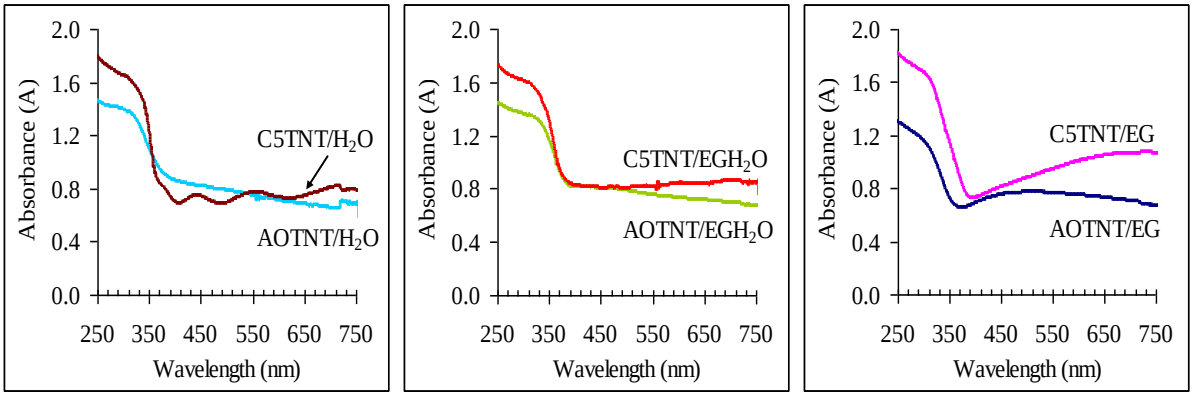

Figure 3. UV-Visible absorbance spectra of TNT/H_2O, TNT/EGH_2O and TNT/EG sample

In addition, the absorbency of visible light (< 550 nm) is higher for C5TNT/EG sample, which could mean that it possesses a higher efficiency of sunlight utilization compared to C5TNT/H_2O and C5TNT/EGH_2O sample. It is thus

expected that C5TNT/EG sample will result in an improvement in solar cell fabrication and in photocatalytic activity. Red shift in absorption wavelength in the visible region for C5TNT/EG might due to oxidation of ethylene glycol to carbonate type species which get adsorbed on the nanotube walls as an outer layer. Sohn et al. [9] also observed the introduction of carbon into TNT, which facilitates the improvement in visible light absorbance when employing ethylene glycol as electrolyte.

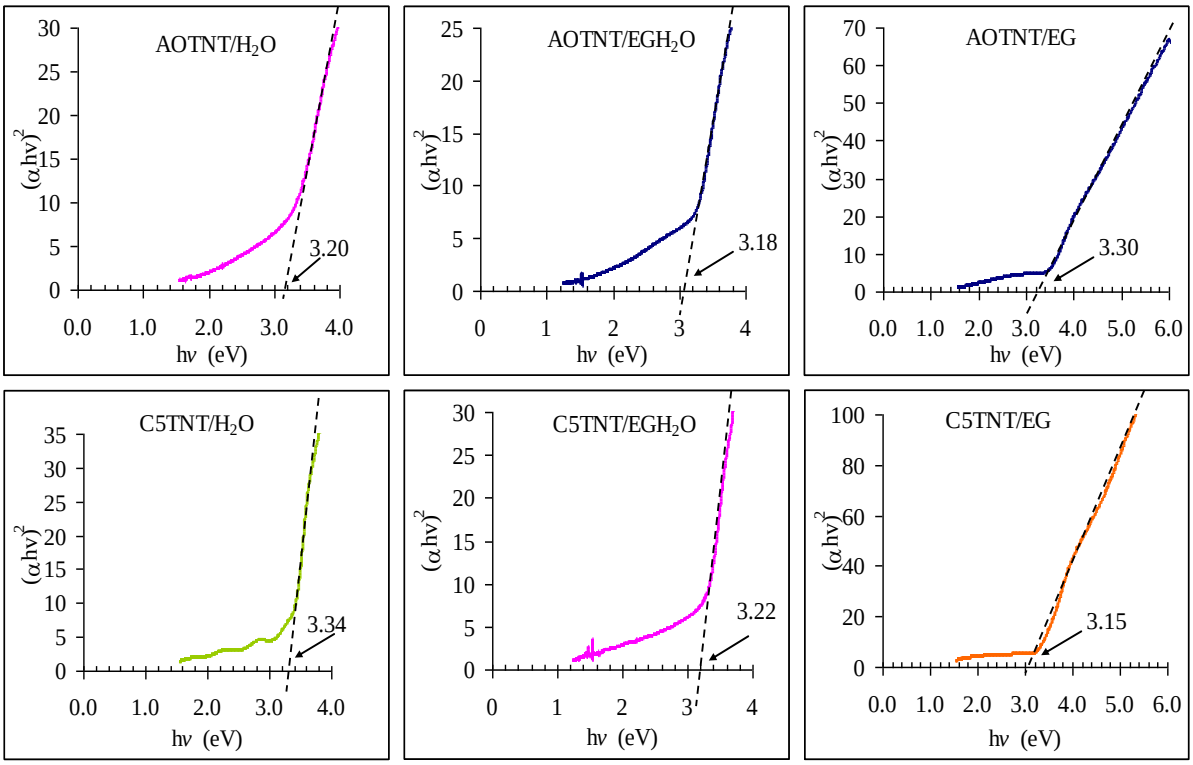

Figure 4. Plot of $(\alpha h\nu)^2$ versus $h\nu$ for AOTNT/H_2O, AOTNT/EGH_2O and AOTNT/EG and their calcined counterparts

Figure 4 shows the plot of $(\alpha h\nu)^2$ versus $h\nu$ for TNT prepared in different electrolytic medium. All the three as-anodised samples, AOTNT/H_2O, AOTNT/EGH_2O and AOTNT/EG have band gap energy of 3.18 – 3.30 eV with a direct transition and this result is similar with the work reported by Song et al. [10]. For the calcined samples, C5TNT/H_2O has the highest direct band gap of 3.34, which was higher than 3.2 eV for bulk anatase due to quantization effect of the nanosized titania. However, C5TNT/EGH_2O and C5TNT/EG exhibited a direct bandgap of 3.22 and 3.15 eV respectively, which was comparable to that of bulk anatase. The calcined samples demonstrated higher band gap than their as-anodised counterpart except for C5TNT/EG sample. From the EDX analysis (Table 2), no carbon was found for both the AOTNT/H_2O and AOTNT/EGH_2O samples whereas a 2.33 wt.% carbon content was found for AOTNT/EG sample.

The photocurrent generated by unmodified Ti and all as-anodized samples (AOTNT/H_2O, AOTNT/EGH_2O and AOTNT/EG) was almost negligible (~2 $\mu A/cm^2$) as they are amorphous without heat treatment. Therefore, the efficiency of generating photocurrent under halogen and UV lamp illumination in methyl orange was compared for all C5TNT/H_2O, C5TNT/EGH_2O and C5TNT/EG samples as shown in Figure 5. Apparently, the photocurrent generated for all samples illuminated with UV lamp was much higher than that observed with halogen lamp, demonstrating that the light from UV lamp (365 nm, 11 mW/m^2) is more efficient in generating and promoting the

electron-hole pairs activity than a halogen lamp (150 mW/m^2). Though halogen lamp exhibits higher photointensity, however, most of the light is given out as heat instead of promoting electron-hole activity. From the DR UV-Vis analysis as shown in Figure 4, the band gap energy for C5TNT/H_2O, C5TNT/EGH_2O and C5TNT/EG is 3.34, 3.22 and 3.15 eV, respectively. Therefore, the light from the UV lamp contains more number of photons with energy exceeding the band gap of TNT, and thus it can excite the TNT samples better compared to halogen lamp. Even though UV rays have higher energies than the light from halogen lamp, the hazardous effects possess by UV radiation is the draw back for the usage of such lamp in activating TNT.

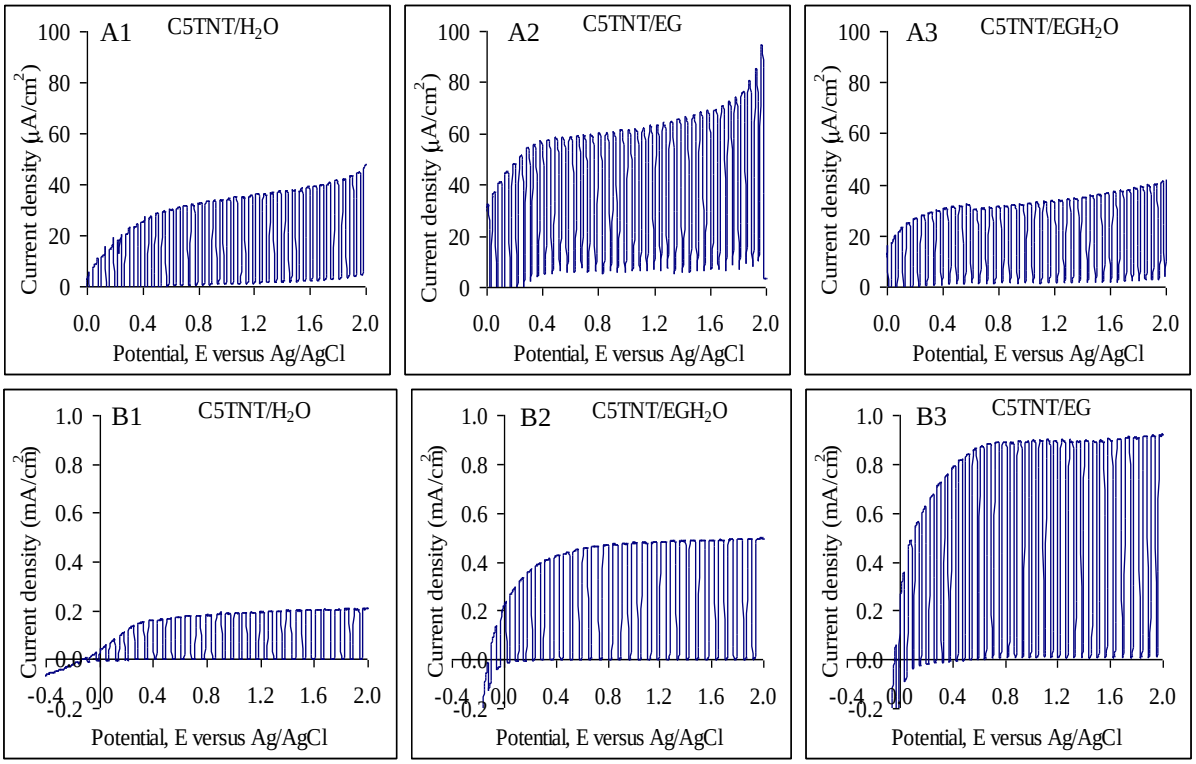

Figure 5. Comparison of the photocurrent potential curve for C5TNT/H_2O, C5TNT/EGH_2O and C5TNT/EG under illumination of halogen lamp (A) and UV lamp (B) in 50 mL 10 ppm methyl orange with 0.1 M KCl as supporting electrolyte

Table 3 shows the dimensional data and photocurrent current for TNT synthesized in different electrolytic medium when illuminated with UV lamp. The magnitude of photocurrent correlates to the efficiency of holes transfer at the oxide-electrolyte interface and electrons transport through nanotubes to the Ti substrate. The lowest photocurrent generated was found for C5TNT/H_2O and a twofold increase on the magnitude of photocurrent was observed for C5TNT/EGH_2O and the highest photocurrent was recorded for C5TNT/EG. Higher photocurrent response obtained for C5TNT/EG sample clearly indicates improved charge separation and greater electrons transport for sample with longer length and larger diameter tubes. In addition, longer length tubes also demonstrated greater surface areas that enhance the absorption of the incident photon, which in return increase the photocurrent response. However, the magnitude of photocurrent did not increase linearly with increasing length as the light intensity usually attenuates as it penetrates into the nanotubes. If the nanotubes have longer length than the effective depth of light penetration, the amount of incident photon absorb by the lower part of nanotubes will be lesser than that by the upper part. Therefore, light absorption by the TNT film will not increase further when the tube length exceeds a certain range.

Table 3. Dimensional data and photocurrent of TNT prepared in different electrolytic medium

Sample	Diameter (nm)	Length (μm)	Photocurrent[a] (mA/cm^2)
C5TNT/H_2O	75 ± 9	0.4 ± 0.01	0.16
C5TNT/EGH_2O	99 ± 10	2.6 ± 0.1	0.47
C5TNT/EG	141 ± 13	11.2 ± 0.3	0.79

[a] *Photocurrent is measured at 0.5 V versus Ag/AgCl in 10 ppm methyl orange solution*

Photoconversion efficiency, η% of light energy to chemical energy in the presence of an external applied potential for different nanotubes was calculated using Equation (2).

$$\eta\% = j_{ph} \left(\frac{[E^{o}_{rev} - |E_{app}|]}{I_o} \right) \times 100 \quad (2)$$

where I_o is the power density of the incident light (mW/cm^2), j_{ph} is the photocurrent density (mA/cm^2), E^{o}_{rev} is the standard reversible potential for water splitting reaction which is 1.23 V versus NHE and the applied potential, $E_{app} = E_{meas} - E_{aoc}$, where E_{meas} is the electrode potential (versus Ag/AgCl) of the working electrode at which photocurrent was measured under illumination and was taken as 0.5 V versus Ag/AgCl in this study. E_{aoc} is the electrode potential (versus Ag/AgCl) of the same working electrode under open circuit conditions, under the same illumination, and in the same electrolyte as shown in Table 4.

Table 4. Photoelectrochemical data and photoconversion efficiency of TNT prepared in different electrolytic medium

Sample	Photocurrent[a] (mA/cm^2)	E_{aoc} (mV)	Photoconversion efficiency (%)
C5TNT/H_2O	0.13	–435	0.49
C5TNT/EGH_2O	0.52	–550	1.23
C5TNT/EG	1.04	–539	2.79

[a]*Photocurrent was done in 0.1 M KOH at 0.5 V versus Ag/AgCl*

As the solar cell parameters such as open circuit potential and short circuit current are best obtained from a non-potentiostated cell configuration, therefore the assessing of the photoefficiency and the use of Equation 2 are only meant to afford figure-of-merit estimates. As shown in Table 4, the highest photoconversion efficiency was obtained for C5TNT/EG in agreement with the highest photocurrent density. Long nanotubes with ordered and well-defined morphology are necessary for good photoelectrochemical performance. The nanotube length obtained for C5TNT/EG is 11.2 μm, which is much longer than that for C5TNT/EGH_2O and C5TNT/H_2O and therefore showed a higher photoefficiency. Other researchers have reported higher photoefficiency with nanotubes length reaching up to 220 μm. For example, Mor et al. [11] had demonstrated that a photoconversion efficiency of 6.8 % was obtained for nanotubes formed in mixture of HF and acetic acid under UV illumination (337 nm). Later, TNT of 6 μm length, under a similar illumination shows a photoconversion efficiency of about 12.25 % [12]. 14.4 μm long TNT fabricated using a formamide-based electrolyte had achieved a photoconversion efficiency of 14.42 % and increased to 16.26 % for 24 μm long TNT fabricated in an ethylene glycol based electrolyte [13]. Nevertheless, it has been reported that the photoefficiency increased with increasing nanotube length up to 5 μm and thereafter tending toward a plateau [14]. Gratzel-type solar cells were fabricated after dye sensitizing the nanotubes layers. The

greatest overall light to electricity conversion efficiency reported for dye-sensitized solar cells based on the nanoparticles TiO_2 have achieved 11% [15]. For pure nanotubes layer, the record efficiency stands at 5.2 % [16] and 7 % for nanotube/nanoparticles mixtures [17].

Conclusion

In summary, titania nanotube arrays were successfully synthesized via electrochemical anodization of Ti in various electrolytic compositions. Choice of electrolytic composition has an effect on the microstructure, element composition, band gap and crystal structure of TNT. In addition, photocurrent response is enhanced using the calcined nanotubes and is affected by the morphology, dimensional changes; with higher photocurrent and photoefficiency conversion is associated with smooth and longer length tube. Highest efficiency was obtained for TNT/EG than those prepared in aqueous solution.

Acknowledgement

This material is based upon work supported by the Malaysia Toray Science Foundation through S&T research grant no. 100-RMI/PRI 16/6/2 (7/2014) and the Ministry of Education through FRGS grant no. 600-RMI/FRGS 5/3 (1/2014). The authors would also like to acknowledge Faculty of Applied Sciences, Universiti Teknologi MARA (UiTM) for the facilities provided.

References

1. Jen, H. P., Lin, M. H., Li, L. L., Wu, H. P., Huang, W. K., Cheng, P. J. and Diau, E. W. G. (2013). High-performance large-scale flexible dye-sensitized solar cells based on anodic TiO_2 nanotube arrays. *ACS Materials & Interfaces*, *5*(20), 10098 – 10104.
2. Yu, M., Long, Y. Z., Sun, B. and Fan, Z. (2012). Recent advances in solar cells based on one-dimensional nanostructure arrays. *Nanoscale*, *4*(9), 2783 – 2796.
3. Smith, Y. R., Sarma, B., Mohanty, S. K. and Misra, M. (2013). Single-step anodization for synthesis of hierarchical TiO_2 nanotube arrays on foil and wire substrate for enhanced photoelectrochemical water splitting. *International Journal of Hydrogen Energy*, *38*(5), 2062 – 2069.
4. Liu, Y., Cheng, Y., Chen, K., Yang, G., Peng, Z., Bao, Q. and Chen, W. (2014). Enhanced light-harvesting of the conical TiO_2 nanotube arrays used as the photoanodes in flexible dye-sensitized solar cells. *Electrochimica Acta*. 146: 838 – 844.
5. Masuda, H. and Fukuda, K. (1995). Ordered metal nanohole arrays made by a two-step replication of honeycomb structures of anodic alumina. *Science* 268(5216):1466 – 1468.
6. Ruan, C., Paulose, M., Varghese, O. K., Mor, G. K. and Grimes, C. A. (2005). Fabrication of highly ordered TiO_2 nanotube arrays using an organic electrolyte. *Journal Physical Chemistry B* 109(33):15754 – 15759.
7. Anitha, V. C., Menon, D., Nair, S. V. and Prasanth, R. (2010). Electrochemical tuning of titania nanotube morphology in inhibitor electrolytes. *Electrochimica Acta* 55(11):3703 – 3713.
8. Sreekantan, S., Saharudin, K., Lockman, Z. and Tzu, T. (2010). Fast-rate formation of TiO_2 nanotube arrays in an organic bath and their applications in photocatalysis. *Nanotechnology* 21:365603.
9. Sohn, Y. S., Smith, Y. R., Misra, M. and Subramanian, V. (2008). Electrochemically assisted photocatalytic degradation of methyl orange using anodized titanium dioxide nanotubes. *Applied Catalysis B: Environmental* 84(3-4):372 – 378.
10. Song, X. M., Wu, J. M. and Yan, M. (2009). Photocatalytic degradation of selected dyes by titania thin films with various nanostructures. *Thin Solid Films* 517(15):4341 – 4347.
11. Mor, G. K., Shankar, K., Paulose, M., Varghese, O. K. and Grimes, C. A. (2005). Enhanced photocleavage of water using titania nanotube arrays. *Nano Letters* 5(1):191 – 195.
12. Shankar, K., Mor, G. K., Prakasam, H. E., Yoriya, S., Paulose, M., Varghese, O. K. and Grimes, C. A. (2007). Highly ordered TiO_2 nanotube arrays up to 220 μm in length: Use in water photoelectrolysis and dye-sensitized solar cells. *Nanotechnology* 18(6):065707.
13. Paulose, M., Prakasam, H. E., Varghese, O. K., Peng, L., Popat, K. C., Mor, G. K., Desai, T. A. and Grimes, C. A. (2007). TiO_2 nanotube arrays of 1000 μm length by anodization of titanium foil: Phenol red diffusion. *Journal Physical Chemistry C* 111(41):14992 – 14997.

14. Watcharenwong, A., Chanmanee, W., de Tacconi, N. R., Chenthamarakshan, C. R., Kajitvichyanukuk, P. and Rajeshwar, K. (2007). Self-organized TiO_2 nanotube arrays by anodization of Ti substrate: Effect of anodization time, voltage and medium composition on oxide morphology and photoelectrochemical response. *Journal Material Research* 22(11):3186 – 3195.
15. Nazeeruddin, M. K., De Angelis, F., Fantacci, S., Selloni, A., Viscardi, G., Liska, P., Ito, S., Takeru, B. and Grätzel, M. (2005). Combined Experimental and DFT-TDDFT Computational Study of Photoelectrochemical Cell Ruthenium Sensitizers. *Journal American Chemical Society,* 127(48):16835 – 16847.
16. Roy, P., Albu, S. P. and Schmuki, P. (2010). TiO_2 nanotubes in dye-sensitized solar cells: Higher efficiencies by well-defined tube tops. *Electrochemistry Communications,* 12(7):949 – 951.
17. HyeokáPark, J. and GuáKang, M. (2008). Growth, detachment and transfer of highly-ordered TiO_2 nanotube arrays: use in dye-sensitized solar cells. *Chemical Communications,* (25):2867 – 2869.